Naval Research Laboratory

Washington, DC 20375-5000

NRL Memorandum Report 6159

Propagation of Charged Particle Beams in the Atmosphere

MARTIN LAMPE

Plasma Theory Branch
Plasma Physics Division

March 4, 1988

SECURITY CLASSIFICATION OF THIS PAGE

REPORT DOCUMENTATION PAGE

Form Approved OMB No. 0704-0188

1a. REPORT SECURITY CLASSIFICATION UNCLASSIFIED	1b. RESTRICTIVE MARKINGS
2a. SECURITY CLASSIFICATION AUTHORITY	3. DISTRIBUTION/AVAILABILITY OF REPORT Approved for public release; distribution unlimited.
2b. DECLASSIFICATION/DOWNGRADING SCHEDULE	
4. PERFORMING ORGANIZATION REPORT NUMBER(S) NRL Memorandum Report 6159	5. MONITORING ORGANIZATION REPORT NUMBER(S)
6a. NAME OF PERFORMING ORGANIZATION Naval Research Laboratory 6b. OFFICE SYMBOL (If applicable) Code 4790	7a. NAME OF MONITORING ORGANIZATION
6c. ADDRESS (City, State, and ZIP Code) Washington, DC 20375-5000	7b. ADDRESS (City, State, and ZIP Code)
8a. NAME OF FUNDING/SPONSORING ORGANIZATION DARPA 8b. OFFICE SYMBOL (If applicable)	9. PROCUREMENT INSTRUMENT IDENTIFICATION NUMBER
8c. ADDRESS (City, State, and ZIP Code) Arlington, VA 22209	10. SOURCE OF FUNDING NUMBERS PROGRAM ELEMENT NO. 62707E PROJECT NO. N60921-86-WR-W023 TASK NO. ARPA Order 4395,A63 WORK UNIT ACCESSION NO. DN680-415

11. TITLE (Include Security Classification)
Propagation of Charged Particle Beams in the Atmosphere

12. PERSONAL AUTHOR(S)
Lampe, Martin

13a. TYPE OF REPORT	13b. TIME COVERED	14. DATE OF REPORT (Year, Month, Day)	15. PAGE COUNT
Interim	FROM _____ TO _____	1988 March 4	31

16. SUPPLEMENTARY NOTATION

17. COSATI CODES			18. SUBJECT TERMS (Continue on reverse if necessary and identify by block number)
FIELD	GROUP	SUB-GROUP	Charged particle beams; Propagation of CPB Relativistic electron beams; Beam propagation

19. ABSTRACT (Continue on reverse if necessary and identify by block number)

We shall review the basic physical processes involved in charged particle beam propagation, in a self-pinched mode, in the atmosphere or other dense neutral gases. These processes include single-particle collisional and radiative energy losses, collective energy loss, radial expansion due to scattering, and instabilities. Each of these imposes requirements and limitations on beam propagation. We shall concentrate on highly relativistic electron beams. Ion beam physics is similar but more complex (because ultra-relativistic approximations are inappropriate), and has been less studied.

Keywords:

20. DISTRIBUTION/AVAILABILITY OF ABSTRACT	21. ABSTRACT SECURITY CLASSIFICATION
☒ UNCLASSIFIED/UNLIMITED ☐ SAME AS RPT. ☐ DTIC USERS	UNCLASSIFIED
22a. NAME OF RESPONSIBLE INDIVIDUAL Martin Lampe	22b. TELEPHONE (Include Area Code) (202) 767-4041 22c. OFFICE SYMBOL Code 4792

DD Form 1473, JUN 86 *Previous editions are obsolete.* SECURITY CLASSIFICATION OF THIS PAGE

S/N 0102-LF-014-6603

CONTENTS

PROPAGATION OF CHARGED PARTICLE BEAMS IN THE ATMOSPHERE

Introduction

This paper presents a brief review of intense relativistic electron beam propagation in "dense" neutral gas. To specify the meaning of "dense", we shall assume that the beam energy is deposited locally and promptly in the gas, resulting in the formation of a highly collisional plasma with electron density n_e low compared to the gas atom density, but high compared to the beam density. These assumptions are usually reasonable for gas densities above a few tens of torr, on up to atmospheric density. This work was originally prepared for the annual Particle Accelerator Conference in Washington, DC, March, 1987, and was constrained in length by the requirements of that conference. It is by no means a complete review of the subject, but I have attempted to present at least a coherent overview. The work reviewed is the product of many investigators; little or no new work is presented here.

A charged particle beam injected into a neutral gas begins immediately to ionize the gas. For example, in air at standard atmospheric density each beam electron collisionally ionizes about 100 thermal electrons per cm. Thus, the "plasma" electron density n_e exceeds the beam density n_b almost immediately. Over a time scale $1/4\pi\sigma$, a very strong radial space charge field expels a small fraction of the plasma electrons, thereby setting up a charge-neutral region within the beam and out to a large radius $b \simeq c/4\pi\sigma$. (Since the plasma is typically weakly ionized and collisional, it can be characterized by a local scalar conductivity σ.)

Manuscript approved November 4, 1987.

Thereafter, the only radial forces on the beam are magnetic: the beam is pinched by its self-force, but this may be partially neutralized by reverse currents induced in the plasma. The beam thus propagates in a self-pinched equilibrium, with the magnetic pinch balancing the beam's transverse pressure, as well as any centrifugal force if the beam is rotating. The equilibrium radius is proportional to the emittance and inversely proportional to the square root of the net (beam plus plasma) current I_n. {If the radial profile of the plasma current $J_p(r)$ differs from that of beam current $J_b(r)$ it is necessary to define an appropriate radially-averaged "effective current" that controls the pinch strength.[1] We shall neglect such subtleties here.} Since I_n generally increases as one moves backward in the beam, the equilibrium has a trumpet-like appearance, with the radius steadily decreasing (Fig. 1a). Indeed, the very front of the beam, where charge neutrality has not been established, is unpinched, has a large radius and constantly erodes due to both radial expansion and energy loss.

Single-Particle Energy Loss

Highly relativistic electrons lose energy, due to ionizing collisions with gas atoms, at a rate given by Bethe's formula,[2,3]

$$dE/dz = -(2\pi nZe^4/mc^2)\ln(\gamma^3 m^2 c^4/2\hbar^2\langle\omega\rangle^2), \qquad (1)$$

where n is the gas atom number density, Z the atomic number, and $\hbar\langle\omega\rangle$ a characteristic bound electron energy. For electrons with $E \gtrsim 1$ MeV in full-density air, this stopping power is 200 to 300 keV/m.

For high-energy electrons (e.g., $\gtrsim$ 100 MeV in air), energy loss due to bremsstrahlung emission dominates. This energy loss process proceeds exponentially, with the **mean** energy $\langle E\rangle$ decreasing as

$$d\langle E\rangle/dz = -\langle E\rangle/\lambda_r, \qquad (2)$$

with the radiation length λ_r given by[2]

$$1/\lambda_r = 4nZ(Z+1)(e^2/\hbar c)(e^2/mc^2)^2 \ln\Lambda, \qquad (3)$$

with $\Lambda \equiv 192/Z^{1/3}$ if $\gamma \gtrsim 100$, or $\Lambda \equiv \gamma$ if $\gamma \lesssim 100$. In standard-density air, $\lambda_r \simeq 300$m. Bremsstrahlung energy loss is statistical in nature, leading to a large energy spread ("straggling"). This has important implications for beam stability and range.[4]

Other single-particle energy loss mechanisms, e.g., synchrotron radiation, are relatively unimportant for beams propagating in air.

Radial Expansion

As a result of multiple small-angle scattering off nuclei, an unpinched electron beam in standard-density air expands as the 3/2 power of distance. This expansion is rapid as compared to energy loss. A pinched beam also expands as its emittance increases by scattering, but in a different and much slower way. Energy loss also has an effect on the beam radius a.

Let us consider a beam which is subject to the energy loss mechanisms discussed above, as well as to multiple small-angle scattering at an angular rate[2]

$$S \equiv d\langle\theta^2\rangle/dz = 16\pi n(Ze^2/\gamma mc^2)^2 \ln(210/Z^{1/3}). \qquad (4)$$

Because neither electron-electron collisions nor bremsstrahlung emission result in angular scattering of a high-energy electron (to within order $1/\gamma$, assumed negligible), it is easily seen that these mechanisms leave the **unnormalized** emittance $\varepsilon \equiv a\sqrt{\langle\theta^2\rangle}$ invariant. If we assume that scattering is slow compared to a betatron oscillation wavelength λ_β of the beam electrons in the pinch potential, i.e., that $\lambda_\beta S/\langle\theta^2\rangle \ll 1$, it can be shown[5] that the beam radial profile assumes a self-similar Bennett profile, and that ε^2 increases at a rate a^2S. In equilibrium, $\langle\theta^2\rangle$ is fixed by Bennett condition,

$$\langle\theta^2\rangle = I_n/I_A, \tag{5}$$

where $I_A \equiv 17\beta\gamma$ kA is the Alfven-Lawson current. Thus, the slow changes in γ (energy loss) and ε (scattering) lead to a steady adiabatic change in a,

$$d\ \ln(\gamma^{-1/2} I_n^{1/2} a)/dz = 1/L_N, \tag{6a}$$

where

$$L_N \equiv (\hbar c/2\pi e^2)(I_n/I_A)\gamma^2\lambda_r. \tag{7}$$

For example, this gives $L_N = (I_n E/7\times10^{12}\text{watts})\lambda_r$ in standard density air. Equations (6),(7) are known as the Nordsieck equation, derived in its basic form (but never published) by A. Nordsieck in the early 1960s. Later contributions were made by Lee.[5,6] Fawley (unpublished recent work) was the first to derive the correct energy dependence in the LHS of (6a).

Energy loss that is due to the effect of E_z electric fields (ohmic loss, to be discussed below) conserves the **transverse** momentum $p_\perp \equiv \gamma m v_\perp$ of each beam electron, and thus, increases the transverse pressure $\langle\gamma n_b m v_\perp^2\rangle$. Ohmic energy loss thus causes beam expansion, whereas it is evident in Eq. (6a) that single-particle energy loss leads to beam contraction. Mathematically, it can be shown that ohmic loss leaves the **normalized** emittance $\gamma\varepsilon$ constant, and that when it predominates the Nordsieck equation takes the form

$$d\ \ln(\gamma^{1/2} I_n^{1/2} a)/dz = 1/L_N. \tag{6b}$$

A few electrons undergo larger-angle single scatterings, which lead to "Moliere scattering".[7] These electrons escape to large radius, and it is simplest to regard them as lost. This leads to a slow decrease in beam current I_b, but to a reduced rate of emittance growth for the remaining beam. The net effect[8] is to increase Eq. (7) for L_N by 20% to 40%, which is in good agreement with experiment.[9]

A beam can only be considered to be pinched, and the Nordsieck equation only applies, if the Nordsieck expansion rate (basically an exponential process with e-folding range L_N) is slower than the diffusive expansion rate for an unpinched beam. This sets a minimum condition for propagation in the pinched mode in a dense medium. It is also to be noted that in air Nordsieck expansion occurs more rapidly than single-particle energy loss if $I_n \lesssim 80$kA and $E \lesssim 100$MeV, or if $I_n E \lesssim 7\times10^{12}$ watts and $E \gtrsim$ 100MeV. It is thus evident that high current and/or energy are necessary for effective self-pinched propagation in dense media.

Energy loss and radial expansion represent fundamental limitations on range, which can be alleviated only by propagating in a reduced-density channel ("hole-boring"). This can be accomplished by sacrificing the front of a particle beam to heat the air and induce radial expansion, which increases the range of the beam tail, or by using a series of beam pulses to produce the same effect, or by using some other means to heat and prepare a reduced-density channel.

Plasma Return Current, Ohmic Loss, and Nose Erosion

Lenz's law suggests that a CPB should induce an axial electric field E_z which opposes the propagation of the beam and drives a reverse current in the conducting medium. E_z extracts energy from the beam and eventually dissipates it in the plasma through resistive decay of the return current. For a highly relativistic beam with $v_z \simeq c$, E_z does not arise at the very front of the beam, where the gas is nonconducting. The fields there are purely transverse electrostatic/magnetostatic. In effect, the beam serves as a guide for an electromagnetic wave (E_r,B_θ) in the vacuum. As σ increases, many things happen in rapid succession at the point where $\zeta \equiv ct-z = c/4\pi\sigma$. ($\zeta$ is the distance behind the beam head, a very useful

coordinate for many purposes.) The beam charge is neutralized and the self-pinch is established. (Hence, this region of the beam is called the "pinch point".) Maxwell's equations reduce to Ampere's law out to a large radius b wherein space charge neutrality prevails. The E_r field "turns around" and becomes an E_z field which is governed by the inductive term in Ampere's law. This leads to a very large spike in the field $E_z(z)$, which can reach many MV/m. As σ continues to increase rapidly, the "monopole" magnetic decay length $c\tau_o \equiv (2\pi\sigma a^2/c)\ln(b/a)$ becomes much larger than the beam radius a and the net current is frozen in. Thereafter E_z takes the value necessary essentially to maintain the value of I_n established at the pinch point. Since σ is rising rapidly, $E_z(\zeta)$ decreases rapidly, making the E_z spike very narrow. Thus, ohmic energy loss extracts energy primarily from beam electrons near the pinch point. Furthermore, ohmic loss results directly in radial expansion, as we have seen. Thus, it is appropriate to regard ohmic loss as primarily a mechanism for erosion of the beam front. If one assumes, for convenience, that the beam current $I_b(\zeta)$ and voltage V are constant, then the ohmic energy loss rate is equivalent to erosion of the beam front at a rate[10,11]

$$d\zeta/dz = (I_n/I_A)\ln(b^2/a^2). \tag{8}$$

We note that nose erosion is additionally driven by scattering, since Nordsieck expansion is fastest at the pinch point, where the pinch force is weak.[10] Scattering-driven erosion is not included in (8).

Calculations[11] also show that if the ionization of the gas is due entirely to beam collisions with gas atoms, then typically I_n settles down to a slowly varying value

$$I_n = I_b/(1+\lambda) \tag{9}$$

shortly behind the pinch point. Here $\lambda \equiv d\tau_1/dt \equiv d(\pi\sigma a^2/2c)/d\zeta$ is a normalized measure of the beam current. The fractional current neutralization $f \equiv -I_p/I_b$ increases with beam current because $d\sigma/d\zeta$ is proportional to I_b/a^2; at higher values of I_b, the effective current is frozen in at an earlier time. For air, and most other simple gases, $I_b \sim 10$kA represents a transition point; higher current beams are mostly current neutralized, while lower current beams are only weakly neutralized.

If I_b rises to its full value over a time long compared the temporal delay from the beam head to the pinch point, then the erosion rate and I_n become functions of the beam rise rate rather than the peak I_b. However, if the beam propagates far enough, the rising portion of $I_b(t)$ eventually erodes away and Eqs. (8) and (9) become directly applicable.

Gas Conductivity

We have already had a number of occasions to refer to the evolution of σ, and this aspect of the physics also has a major effect on beam instabilities. At this point, we shall briefly consider the principal mechanisms that underlie plasma conductivity.

The conductivity may be written $n_e e\mu$, where μ is the electron mobility, determined in general by both electron-neutral (e-n) and electron-ion (Spitzer) collisions. Frequently a dense gas is only weakly ionized by a beam and e-n collisions dominate, in which case μ is independent of n_e and only weakly dependent on temperature T_e (typically, $\mu \propto 1/\sqrt{T_e}$). Thus, σ depends primarily on the ionization and de-ionization processes that control n_e, which increases rapidly from zero to $n_e \gtrsim 10^{16}$. In addition to beam-collisional ionization, avalanche ionization (i.e., ionization of atoms by plasma electrons which have been energized by macroscopic electric fields) may occur, particularly near the pinch point

where large electric fields are present. De-ionization is usually due primarily to recombination, at least within the core of the beam. (In some gases, e.g., O_2, attachment can be important at large radii or wherever n_e is relatively low. This will be ignored here.) We may thus write an equation governing the evolution of σ:

$$d\sigma/d\zeta = \alpha_1(T_e)J_b + \alpha_2(T_e)\sigma - \beta(T_e)\sigma^2. \qquad (10)$$

In the front portion of the beam and out to one or two beam radii, beam-collisional ionization [the first term of (10)] usually dominates, except possibly at the pinch point. In this case (and if we also neglect the T_e-dependence) the radial profile of $\sigma(r)$ is identical to that of $J_b(r)$. Moreover, the plasma current $J_p(r) = \sigma E_z$ has a similar profile, since E_z is only weakly dependent on r within the beam. [See Eq. (11) below.] This approximation is frequently made in analytic studies, and greatly simplifies the analysis. Avalanche [the second term in (10)] has two effects. Avalanche driven by E_z at the pinch point causes the central $\sigma(r)$ profile to become narrower than $J_b(r)$, a destabilizing effect that will be discussed later. Avalanche driven by E_r in the very front of the beam produces a very broad low-level conductivity out to the large radius b, which has important consequences, e.g., the large inductive logarithms in Eq. (8). Further back in the beam, where recombination [the third term of (10)] becomes important, $\sigma(r)$ becomes broader than $J_b(r)$, which helps stability. We note that, in a complex gas such as air, recombination can depend on water vapor content and complicated temperature-dependent chemistry effects, e.g., the formation of molecular complexes.[12] On a practical level, even the weak dependence of μ on T_e can have significant effects, e.g., on hose instability,[13] as discussed below. To model temperature-dependent effects, it is frequently convenient to assume that

(in a diatomic gas) T_e is determined by a balance between ohmic heating and energy loss to vibrational modes of the molecules. In this case, it can be shown that T_e is a function only of E/ρ, where E is the electric field and ρ is the gas density. We can then write the coefficients in Eq. (10) as functions of E/ρ. A summary of these coefficients is given in Refs. 13 and 14.

We have assumed that the plasma conductivity is local, scalar, and is created instantaneously by beam collisions. In fact, beam-gas collisions do create high-energy secondary electrons (delta rays) which have long mean free paths. Although relatively few in number, these secondaries can have some effect in spreading and delaying conductivity, and in responding nonlocally to electric fields. It is also true that tensor conductivity can play some role if the net current is high or the beam radius is small, leading to strong magnetic fields.

Beam Instabilities

As a magnetically confined, highly ordered system, a self-pinched beam is subject to a number of instabilities, which are driven by two effects: (1) If there is a substantial return current $I_p \equiv -fI_b$, then there is a repulsive magnetic force between I_p and I_b. As long as I_p and I_b remain well aligned and more or less proportional to each other, this merely weakens the pinch in an orderly way, but if perturbations lead to a separation of I_p and I_b, the repulsive force can drive unstable growth of the perturbations. This is the primary mechanism for all of the instability modes except hose. Each has a threshold value of f below which the mode is stable.[15] (The hose mode is unstable even if $f = 0$, but is further destabilized by nonzero return current.) (2) Even if $I_p = 0$, symmetry-breaking distortions can drive locally destabilizing magnetic

forces. Finite plasma resistivity plays a key role here. Because $\sigma \neq \infty$, magnetic field lines are not frozen into the plasma, and instabilities can occur on the time scale for beam motion, rather than the much slower hydrodynamic time scale for the plasma. But because $\sigma \neq 0$, the field lines are subject to destabilizing phase lags as they try to follow beam distortions. This mechanism particularly drives the resistive hose instability, which is the most notorious of the beam instabilities.

The linearized normal modes of a beam can be characterized by a pair of quantum numbers (m,n), where m indicates θ-dependence $\exp(im\theta)$, and n is the radial mode number, roughly speaking the number of oscillations within the beam radius. The first few modes, shown in Fig. 1, are the most important for pinched beams: (m = 0, n = 1) is the sausage mode, roughly a self-similar expansion/contraction of the beam; (m = 0, n = 2) is the axisymmetric hollowing mode, in which the beam density alternately hollows out and peaks on axis; (m = 1, n = 0) is the hose mode, in which the beam thrashes around more or less like a firehose, without a great deal of internal distortion. The filamentation modes ($m \geq 2$ or $n \geq 3$) generally have a high threshold value of f[15] and are believed to be stable for pinched beams, except in annular (usually rotating) beam equilibria.

Axisymmetric Hollowing Instability

The axisymmetric hollowing instability was discovered in computer simulations[14] as a particularly violent instability, leading to rapidly growing radial oscillations that destroy the beam only a few nanoseconds behind the pinch point. Computer simulations have provided a detailed, quantitative, and rather surprising picture of its nature. Figure 2 shows the growth of the instability as a function of z and ζ (used as independent variables in place of the usual z and t), and Fig. 3 shows the radial profile $J_b(r,\zeta)$ characteristic of the instability.

Since the simulations show the instability in the large-amplitude nonlinear stage, where large radial oscillations are apparent, it was thought at first that this was basically a sausage instability, although hollowing of the beam profile is apparent in Fig. 3. However, when the beam profile was constrained to a self-similar shape, the instability disappeared, thus indicating that hollowing is an essential feature. Furthermore, a linearized analytic theory of the sausage mode[16] shows that instability is not expected for a beam injected into neutral gas. [Basically this is because beam perturbations create similar conductivity perturbations through Eq. (10). This effect inhibits spatial separation of I_b and I_p, and thus reduces the growth rate for all modes; it just barely suffices to stabilize the sausage mode.] Furthermore, when the avalanche term in Eq. (10) was artificially turned off, the instability disappeared. Finally, it was found that when E/ρ was extremely large (specified below), the instability turned off.

The essence of the hollowing instability is as follows. Behind the pinch point, where Ampere's law (in its axisymmetric form) is valid, one can show that the electric field has the radial profile

$$E_z(r) \propto \ln[(1 + b^2/a^2)/(1 + r^2/a^2)]. \qquad (11)$$

E_z has a weak (logarithmic) maximum on axis, which is usually ignored in analyses. However, over a wide range of parameters, the **exponentiation rate** for avalanche ionization rates increase as a high power (4 to 6) of E/ρ. Thus, σ, and also the plasma return current $J_p = E_z\sigma$, become strongly peaked there, and the repulsive magnetic force hollows out the beam and blows it out to large radius. This expansion reverses itself only because the radial expansion of the beam current decreases the inductance L of the system. Roughly speaking, LI_n tends to be constant, so the defocusing plasma current decreases, or may even reverse itself so as to augment the

pinch.[17,18] The beam current then comes crashing back onto the axis, and the cycle is repeated with rapidly increasing amplitude.

The key quantitative features revealed by the simulations are that the instability occurs, over a wide range of densities, only if two conditions are met. First, $f > 50\%$, in qualitative agreement with prior analytic predictions.[15] This is easily understood: even if the return current flows in a profile that is very narrow compared to the beam current, the pinch is destroyed overall if and only if $J_p > J_b/2$. Secondly, the value of E_z/ρ at the pinch point (in air) must fall into the range

$$13 \text{ MV/m-torr} < E_z/\rho < 50 \text{ MV/m-torr}. \qquad (12)$$

The lower limit on E_z/ρ ensures that avalanche is strong enough to play a significant role. The upper limit is due to the fact that, although avalanche is very strong at large values of E/ρ, it no longer increases rapidly as a function of E/ρ.

In order to avoid the hollowing instability, it is thus necessary to keep the maximum value of E_z below the lower limit of Eq. (12). (In gas at any significant fraction of atmospheric density, the upper limit is not exceeded.) This can be accomplished in several ways: (1) By limiting the rise rate of $I_b(t)$, so that the current at the pinch point is not above a critical value. (2) By limiting the peak value of I_b. Even if $I_b(t)$ rises instantaneously, instability occurs (in air) only if $I_b \gtrsim 20$kA multiplied by the density in atmospheres, for beam radii in the vicinity of 1cm. (3) Increasing the beam radius.

These conclusions were subsequently tested in an experiment performed on the IBEX electron beam facility at Sandia National Laboratories.[19] The hollowing instability was clearly seen to occur at air densities below 80 torr, in quantitative agreement with predictions based on Eq. (12), and to turn off at higher pressures where E_z/ρ became too small.

Hose Instability

The resistive hose instability is the most important impediment to propagation of pinched beams. It is observed in nearly all beam propagation experiments, and has been studied extensively by means of linearized analytic theory as well as both linearized and nonlinear numerical simulations. The analysis indicates that the instability is always present for a pinched beam injected into neutral gas, but that it can be minimized by limiting the beam duration and reducing the level of initial perturbation.

Analytic studies of the hose instability have usually been based on linearized theory for perturbations to an axially uniform beam equilibrium, i.e., $J_{bo}(r,\zeta)$ independent of ζ. Hose normal modes take the form $f(r,\zeta)\exp[i(\theta + \Omega z/c)]$. It may also be assumed that the equilibrium plasma current $J_{po}(r,\zeta)$ and (in the simpler theories) conductivity $\sigma_o(r,\zeta)$ are ζ-independent, in which case the normal mode dependence reduces to $f(r)\exp[i(\theta c + \omega\zeta + \Omega z)/c]$ and a dispersion relation $\omega(\Omega)$ is sought. Effects associated with the beam head and pinch point, e.g., low conductivity, space charge, and incomplete pinch, are usually neglected, and in this spirit the electrodynamics are calculated simply from Ampere's law (exceptions are Refs. 20,21).

The earliest version of hose theory (the "rigid beam" model) assumed in addition that the perturbation of each "slice" of the beam consists of a transverse displacement by an amount $Y\exp[i(\omega\zeta + \Omega z)]$, with no internal distortion. As a nearly exact consequence of the linearized Ampere's law the vector potential $A_z(r,z,\zeta)$ is also displaced from the axis of symmetry, by an amount $D\exp[i(\omega\zeta + \Omega z)]$, without internal distortion. The problem reduces to ODE's,

$$\partial^2 Y/\partial z^2 = \Omega_\beta^2 (D-Y)/c^2 \tag{13}$$

$$D + c\tau_1(\partial D/\partial \zeta) = Y, \tag{14}$$

where $\tau_1 = \pi\sigma a^2/2c^2$ is the "dipole" magnetic decay time. Equations (13) and (14) lead to a dispersion relation

$$i\omega\tau_1 = -\Omega^2/(k_\beta^2 - \Omega^2), \tag{15}$$

which correctly shows that oscillation in z scales to λ_β while growth in ζ scales to the τ_1. However, the infinite growth rate predicted at $\Omega \to k_\beta$, indicative of absolute instability in the beam frame, is incorrect.

The crucial oversimplification in Eqs. (13)-(15) is the implicit assumption that all beam electrons oscillate at a single resonant betatron frequency, i.e., that the potential well pinching the beam is simply harmonic. This would be true for a flat-topped current profile, but the rounded profiles of J_b and J_p introduce anharmonicity, and therefore a dependence of k_β on the amplitude of an electron's orbit. When this feature is introduced into the modeling, as was first done by using the "spread mass" formalism,[22] the dispersion relation exhibits a finite maximum growth rate. For example, Lee[22] finds

$$-i\omega\tau_1 = 3x^2 - 6x^4 + 6(x^4 - x^6)[i\pi + \ln(1/x^2 - 1)], \tag{16}$$

where $x \equiv \Omega^2/\Omega_b^2$. Equation (16) is illustrated in Fig. 4, for a beam with no return current. Most significantly, the instability is convective backward in the beam frame; hence, it reaches a maximum amplitude at any given point in the beam and then decays. Thus, the hose amplitude can be limited by limiting the beam duration to a few growth lengths and by insuring that the beam is initially quiescent, so that hose modes have to e-fold many times.

Subsequent to Lee's pioneering work, hose modeling has been extended in many ways. More sophisticated macroscopic models,[23] linearized Vlasov calculations,[24] and simulations[17,18,23-25] have been used to treat beam dynamics. Plasma return current has been included and found to be strongly destabilizing.[23,24,26] Self-consistent treatment of conductivity evolution introduces a variety of effects. A fully analytic linear theory has been developed which includes the linear increase of equilibrium conductivity $\sigma_o(r,\zeta)$ with ζ due to beam-collisional ionization of the gas; in this case, instability grows as a power p of ζ, rather than exponentially.[24] Since p is inversely proportional to σ_o, growth is most rapid just behind the pinch point. (The formalism is invalid ahead of the pinch point). Furthermore, dipole perturbations of the beam induce dipole perturbations of σ through Eq. (10). This significantly reduces the growth rate in the presence of plasma return current, particularly for low frequency modes, by inhibiting separation of the beam current from the return current.[24] One consequence of this is that the hose growth rate typically decreases with increasing I_b, as shown in Fig. 5. This is the net result of three pieces of physics: (i) $\tau_1 \propto I_b$, which favors higher currents; (ii) the destabilizing effect of current neutralization, which favors lower currents; (iii) the effect of dipole conductivity, which swings the balance to higher currents. Even the T_e-dependence of σ, i.e., the inverse dependence of σ on E/ρ, can be included in a fully analytic theory;[13] since E_z is largest at the pinch point and steadily decreases thereafter, this further accentuates the tendency for hose to grow rapidly at the pinch point and very slowly further back in the beam.

Numerical simulation has been essential to detailed understanding of hose.[17,18,24,25] It permits self-consistent treatment of the radial and ζ dependence of beam equilibria, of phenomena near the pinch point where

Ampere's law is invalid, and of nonlinear effects. Conversely, the hose instability has stimulated the development of innovative simulation models.[24,25] One conclusion from these studies is that avalanche ionization at the pinch point is lethal, strongly driving hose as well as axisymmetric hollowing, and for similar reasons.

Conclusions

We have seen that propagation of beams in dense gases is limited in varying ways by energy loss, radial expansion, nose erosion, and hose and hollowing instabilities. For the most part, these limitations are minimized by going to higher energies and currents, fatter beams, shorter pulses, and beams which are more quiescent at injection.

Acknowledgments

Although many investigators have made major contributions to the study of beam propagation, I am particularly grateful to Drs. Edward P. Lee, Glenn Joyce, and Richard F. Hubbard, whose insights have contributed greatly to my personal understanding of the subject.

This work was supported by DARPA under Contract No. N60921-86-WR-W0233, ARPA Order No. 4395, Amendment 63.

References

1. E. P. Lee, Lawrence Livermore National Laboratory Report UCID-18940, 1981.

2. J. D. Jackson, Classical Electrodynamics, New York: Wiley, 1967, pp. 440, 458, 519.

3. B. Rossi, High Energy Particles, Englewood Cliffs, N. J.: Prentice-Hall, 1952, p. 55.

4. M. I. Haftel, M. Lampe, and J. B. Aviles, Phys. Fluids **22**, 2216-2229, 1979.

5. E. P. Lee, Phys. Fluids **19**, 60, 1976.

6. E. P. Lee and R. K. Cooper, Part. Accel. **7**, 83, 1976.

7. H. A. Bethe, Phys. Rev. **89**, 1256, 1953.

8. T. P. Hughes and B. B. Godfrey, Phys. Fluids **27**, 1531, 1984.

9. R. J. Briggs, R. E. Hester, E. J. Lauer, E. P. Lee, and R. I. Spoerlein, Phys. Fluids **19**, 1007, 1976.

10. E. P. Lee, Lawrence Livermore National Laboratory Report UCID-18768, 1980.

11. W. M. Sharp and M. Lampe, Phys. Fluids **23**, 2383, 1980.

12. A. W. Ali, NRL Memo Report 4617, 1981. ADA105-749

13. S. P. Slinker, R. F. Hubbard, and M. Lampe, J. Appl. Phys. **62**, 1171, 1987.

14. G. Joyce and M. Lampe, Phys. Fluids **26**, 3377, 1983.

15. H. S. Uhm and M. Lampe, Phys. Fluids **25**, 1444, 1982.

16. M. Lampe and G. Joyce, Phys. Fluids **26**, 3371, 1983.

17. B. Hui, R. F. Hubbard, M. Lampe, Y. Y. Lau, R. R. Fernsler, and G. Joyce, Phys. Rev. Lett. **55**, 87, 1985.

18. R. F. Fernsler, R. F. Hubbard, B. Hui, G. Joyce, M. Lampe, and Y. Y. Lau, Phys. Fluids **29**, 3056, 1986.

19. C. A. Ekdahl, J. R. Freeman, G. J. Leifeste, R. B. Miller, W. B. Stygar, and B. B. Godfrey, Phys. Rev. Lett. **55**, 935, 1985.

20. E. P. Lee, Lawrence Livermore National Laboratory Report UCID 16734, 1975.

21. H. S. Uhm and M. Lampe, Phys. Fluids **24**, 1553, 1981.

22. E. P. Lee, Phys. Fluids **21**, 1327, 1978.

23. W. M. Sharp, M. Lampe, and H. S. Uhm, Phys. Fluids **25**, 1456, 1982.

24. M. Lampe, W. M. Sharp, R. F. Hubbard, E. P. Lee, and R. J. Briggs, Phys. Fluids **27**, 2821, 1984.

25. G. Joyce and M. Lampe, J. Comp. Phys. **63**, 398, 1986.

26. H. S. Uhm and M. Lampe, Phys. Fluids **23**, 1574, 1980.

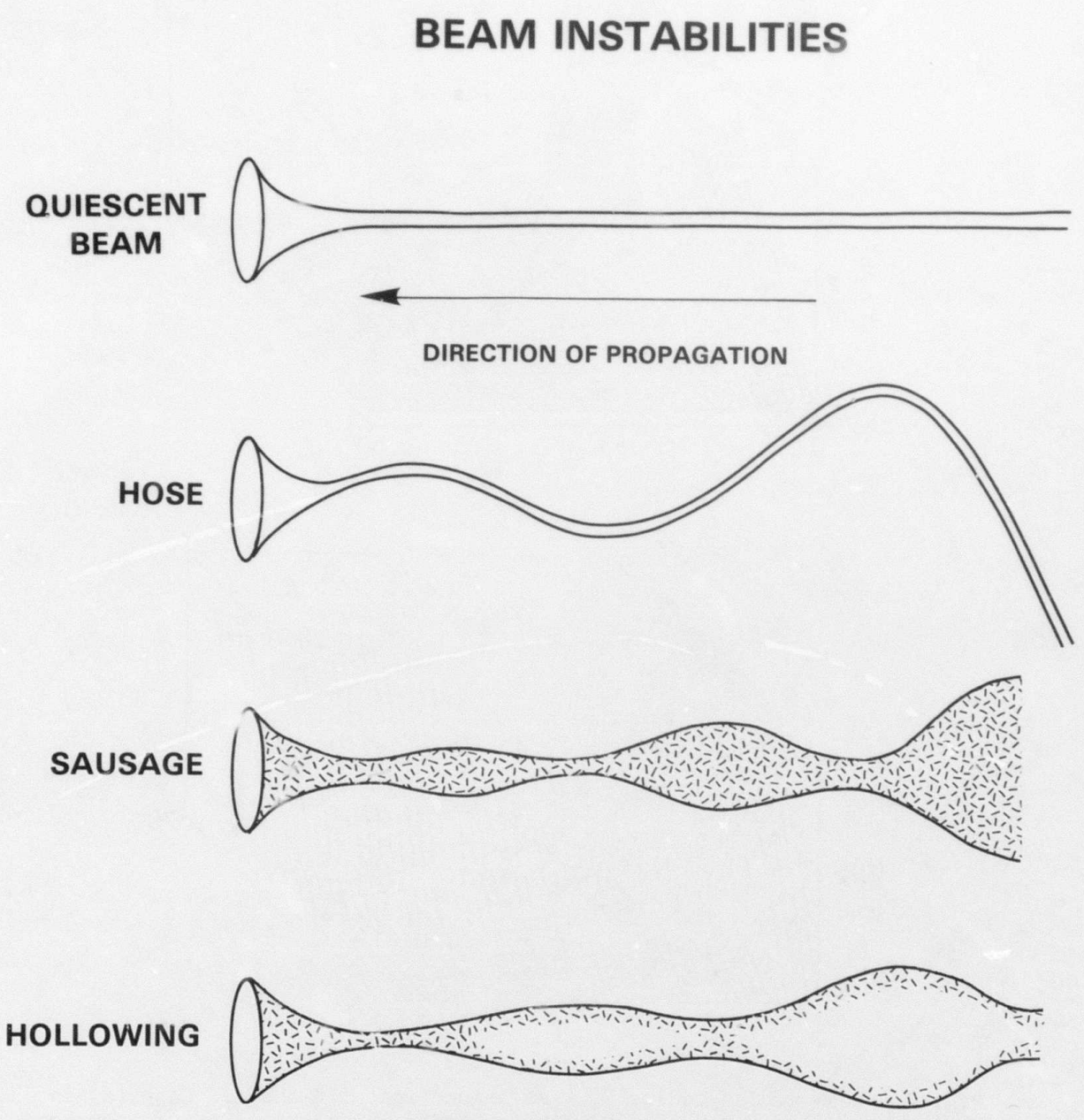
BEAM INSTABILITIES
QUIESCENT BEAM
DIRECTION OF PROPAGATION
HOSE
SAUSAGE
HOLLOWING

Fig. 1.

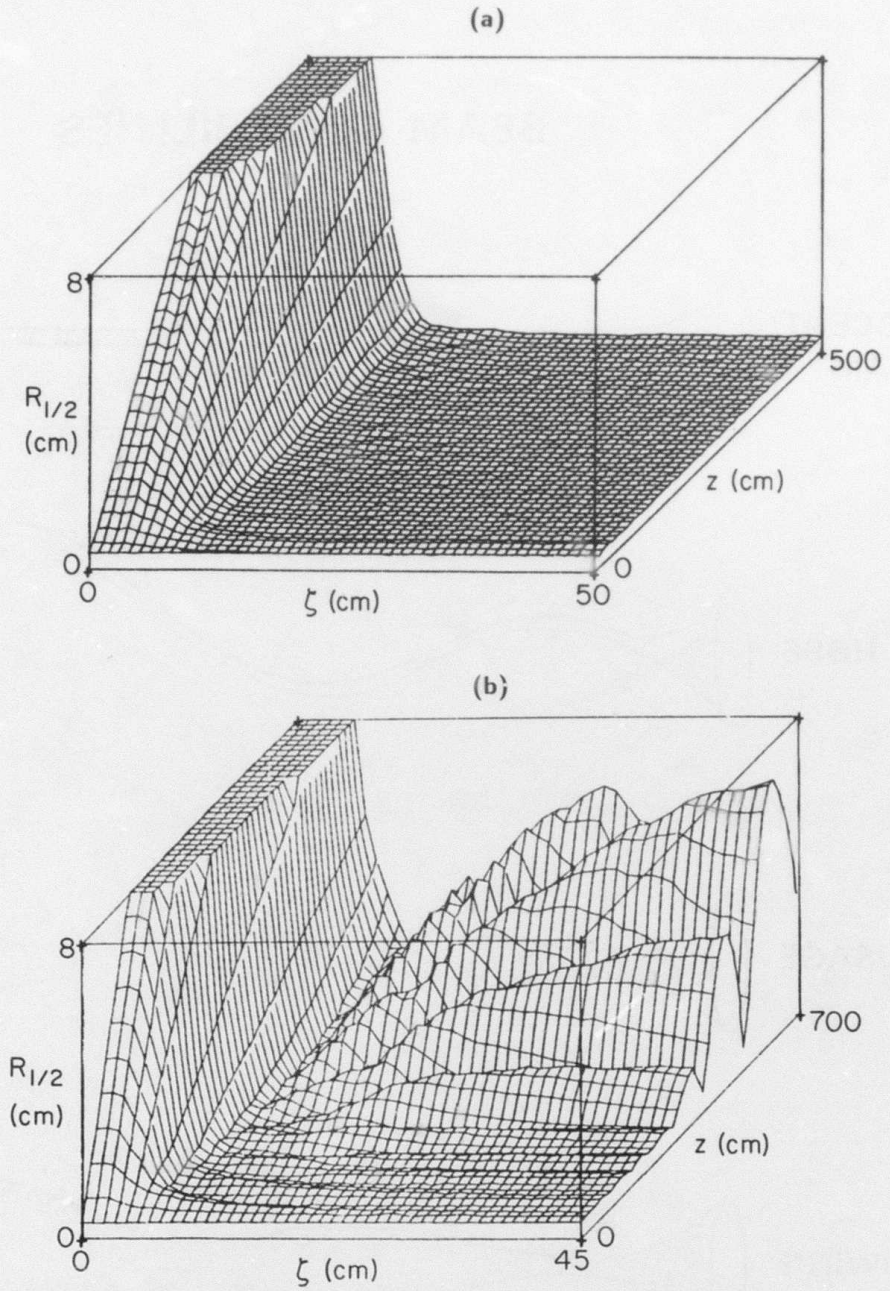

Fig. 2. Beam median radius $R_{1/2}$ as a function of ζ and z. Case (a) is stable, and shows only the expanded and slowly eroding beam head. Case (b) is unstable, and shows the large radial oscillations characteristic of the hollowing instability. (From Ref. 14.)

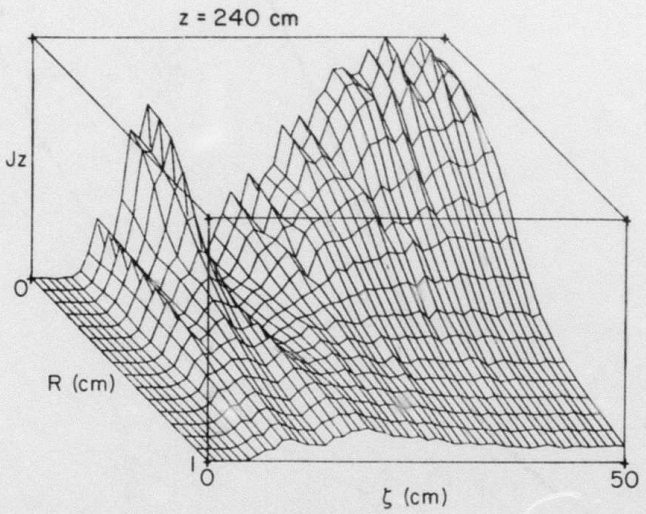

Fig. 3. Beam current density as a function of ζ (the distance behind the beam head) for fixed z, showing hollowing and peaking. (From Ref. 14.)

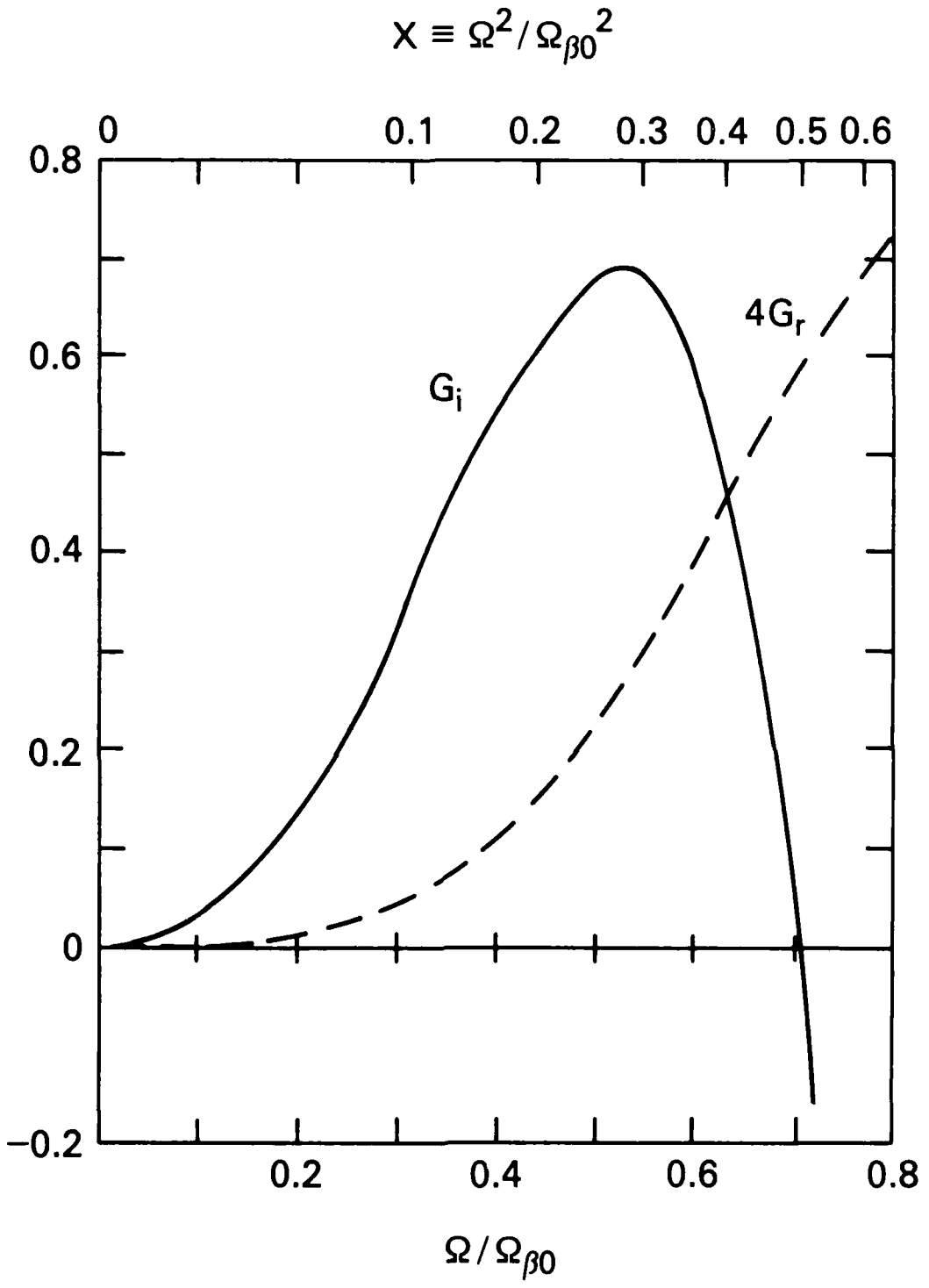

Fig. 4. Dispersion relation for hose instability from the spread mass model.

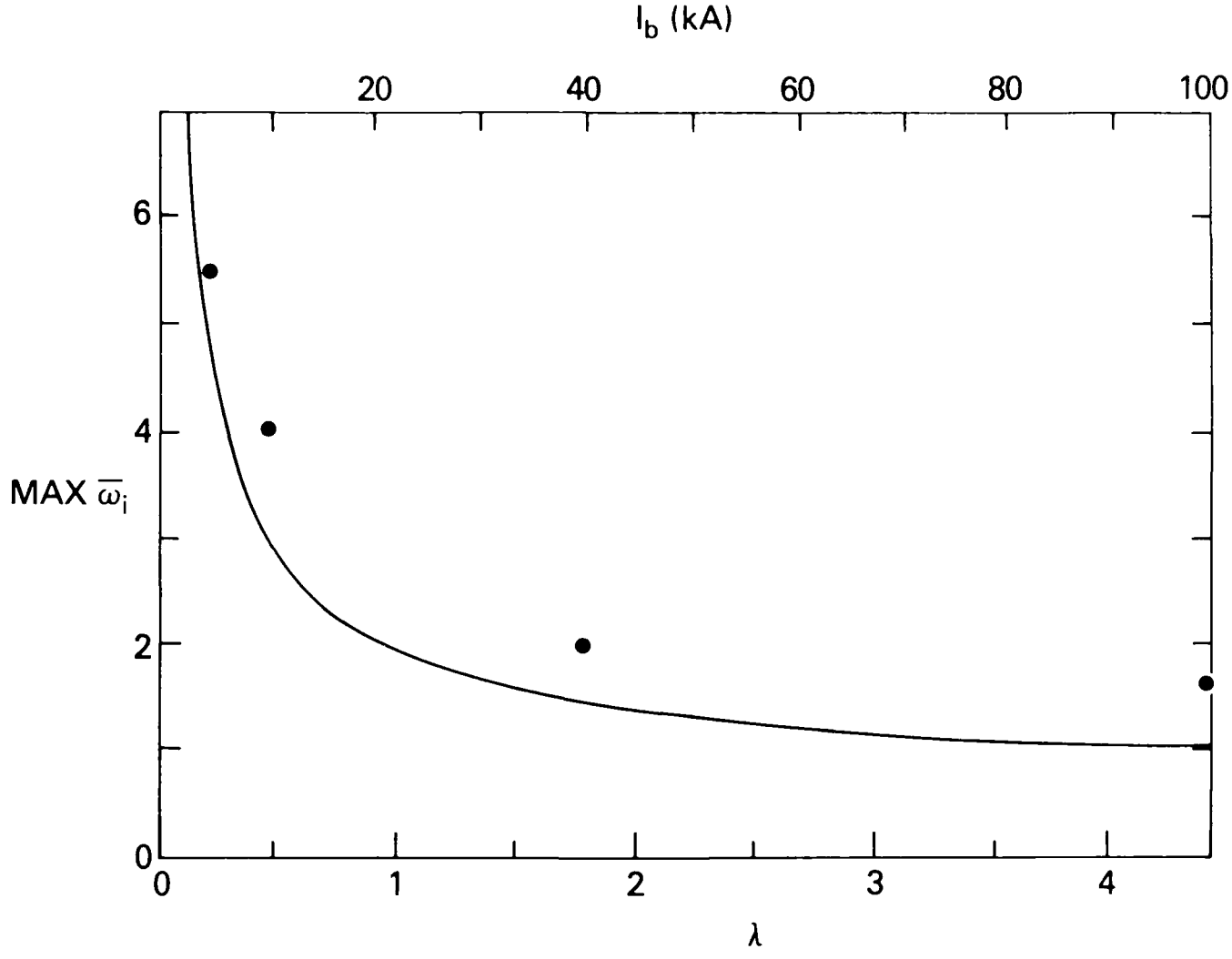

Fig. 5. Peak hose growth rate as a function of beam current. The curve is an analytic result from Ref. 24, while the dots are the result of simulations with the multi-component code VIPER, also taken from Ref. 24.

Distribution List*

Naval Research Laboratory
4555 Overlook Avenue, S.W.
Attn: CAPT W. G. Clautice - Code 1000
Dr. M. Lampe - Code 4792 (20 copies)
Dr. T. Coffey - Code 1001
Head, Office of Management & Admin - Code 1005
Director of Technical Services - Code 2000
NRL Historian - Code 2604
Dr. J. Boris - Code 4040
Dr. M. Picone - Code 4040
Dr. M. Rosen - Code 4650
Dr. M. Haftel - Code 4665
Dr. S. Ossakow - Code 4700 (26 copies)
Dr. A. Ali - Code 4700.1
Dr. M. Friedman - Code 4700.1
Dr. R. Taylor - BRA (4700.1)
Mr. I. M. Vitkovitsky - Code 4701
Dr. S. Gold - Code 4740
Dr. R. Meger - Code 4750
Dr. A. Robson - Code 4760
Dr. D. Murphy - Code 4763
Dr. R. Pechacek - Code 4763
Dr. D. Taggart - Code 4763
Dr. G. Cooperstein - Code 4770
Dr. D. Colombant - Code 4790
Dr. R. Fernsler - Code 4790
Dr. I. Haber - Code 4790
Dr. R. F. Hubbard - Code 4790
Dr. G. Joyce - Code 4790
Dr. Y. Lau - Code 4790
Dr. S. P. Slinker - Code 4790
Dr. P. Sprangle - Code 4790
W. Brizzi - Code 4790A
Code 4790 (20 copies)
Library - Code 2628 (2 copies)
D. Wilbanks - Code 2634
Code 1220

Air Force Office of Scientific Research
Physical and Geophysical Sciences
Bolling Air Force Base
Washington, DC 20332
Attn: Major Bruce Smith

Air Force Weapons Laboratory
Kirtland Air Force Base
Albuquerque, NM 87117
Attn: W. Baker (AFWL/NTYP)
D. Dietz (AFWL/NTYP)
Lt Col J. Head

U. S. Army Ballistics Research Laboratory
Aberdeen Proving Ground, Maryland 21005
Attn: Dr. Donald Eccleshall (DRXBR-BM)
Dr. Anand Prakash

Avco Everett Research Laboratory
2385 Revere Beach Pkwy
Everett, Massachusetts 02149
Attn: Dr. R. Patrick
Dr. Dennis Reilly

Ballistic Missile Def. Ad. Tech. Ctr.
P.O. Box 1500
Huntsville, Alabama 35807
Attn: Dr. M. Hawie (BMDSATC-1)

Chief of Naval Material
Office of Naval Technology
MAT-0712, Room 503
800 North Quincy Street
Arlington, VA 22217
Attn: Dr. Eli Zimet

Cornell University
369 Upson Hall
Ithaca, NY 14853
Attn: Prof. David Hammer

DASIAC - DETIR
Kaman Tempo
25600 Huntington Avenue, Suite 500
Alexandria, VA 22303
Attn: Mr. F. Wimenitz

Defense Advanced Research Projects Agency
1400 Wilson Blvd.
Arlington, VA 22209
Attn: Dr. Shen Shey
Dr. H. L. Buchanan

Department of Energy
Washington, DC 20545
Attn: Dr. Wilmot Hess (ER20:GTN,
High Energy and Nuclear Physics)
Mr. Gerald J. Peters (G-256)

Directed Technologies, Inc.
8500 Leesburg Pike, Suite 601
Vienna, VA 22180
Attn: Dr. Ira F. Kuhn
Dr. Nancy Chesser

C. S. Draper Laboratories
555 Technology Square
Cambridge, Massachusetts 02139
Attn: Dr. E. Olsson
Dr. L. Matson

General Dynamics Corporation
Pomana Division
1675 W. Mission Blvd.
P. O. Box 2507
Pomana, CA 92769-2507
Attn: Dr. Ken W. Hawko

Hy-Tech Research Corp.
P. O. Box 3422 FSS
Radford, VA 24143
Attn: Dr. Edward Yadlowsky

HQ Foreign Technology Division
Wright-Patterson AFB, OH 45433
Attn: TUTD/Dr. C. Joseph Butler

Institute for Fusion Studies
University of Texas at Austin
RLM 11.218
Austin, TX 78712
Attn: Prof. Marshall N. Rosenbluth

Intelcom Rad Tech.
P.O. Box 81087
San Diego, California 92138
Attn: Dr. W. Selph

Joint Institute for Laboratory
Astrophysics
National Bureau of Standards and
University of Colorado
Boulder, CO 80309
Attn: Dr. Arthur V. Phelps

Kaman Sciences
1500 Garden of the Gods Road
Colorado Springs, CO 80933
Attn: Dr. John P. Jackson

La Jolla Institute
P. O. Box 1434
La Jolla, CA 92038
Attn: Dr. K. Brueckner

Lawrence Berkeley Laboratory
University of California
Berkeley, CA 94720
Attn: Dr. Edward P. Lee

Lawrence Livermore National Laboratory
University of California
Livermore, California 94550
Attn: Dr. Richard J. Briggs
Dr. Simon S. Yu
Dr. Frank Chambers
Dr. James W.-K. Mark, L-477
Dr. William Fawley
Dr. William Barletta
Dr. William Sharp
Dr. Daniel S. Prono
Dr. John K. Boyd
Dr. Kenneth W. Struve
Dr. John Clark
Dr. George J. Caporaso
Dr. William E. Martin
Dr. Donald Prosnitz

Lockheed Missiles and Space Co.
3251 Hanover St.
Bldg. 205, Dept 92-20
Palo Alto, CA 94304
Attn: Dr. John Siambis

Los Alamos National Scientific Laboratory
P.O. Box 1663
Los Alamos, NM 87545
Attn: Dr. L. Thode
Dr. H. Dogliani, MS-5000
Dr. R. Carlson
Ms. Leah Baker, MS-P940
Dr. Carl Ekdahl
Dr. Joseph Mack

Maxwell Laboratories Inc.
8888 Balboa Avenue
San Diego, CA 92123
Attn: Dr. Ken Whitham

McDonnell Douglas Research Laboratories
Dept. 223, Bldg. 33, Level 45
Box 516
St. Louis, MO 63166
Attn: Dr. Evan Rose
Dr. Carl Leader
Dr. Frank Bieniosek

Mission Research Corporation
1720 Randolph Road, S.E.
Albuquerque, NM 87106
Attn: Dr. Brendan Godfrey
Dr. Thomas Hughes
Dr. Lawrence Wright
Dr. Barry Newberger
Dr. Michael Mostrom
Dr. Dale Welch

Mission Research Corporation
P. O. Drawer 719
Santa Barbara, California 93102
Attn: Dr. C. Longmire
Dr. N. Carron

National Bureau of Standards
Gaithersburg, Maryland 20760
Attn: Dr. Mark Wilson

Naval Surface Warfare Center
White Oak Laboratory
Silver Spring, Maryland 20903-5000
Attn: Dr. R. Cawley
Dr. J. W. Forbes
Dr. B. Hui
Mr. W. M. Hinckley
Mr. N. E. Scofield
Dr. E. C. Whitman
Dr. M. H. Cha
Dr. H. S. Uhm
Dr. R. Fiorito
Dr. K. T. Nguyen
Dr. R. Stark
Dr. R. Chen
Dr. D. Rule

Office of Naval Research
800 North Quincy Street
Arlington, VA 22217
Attn: Dr. C. W. Roberson
Dr. F. Saalfeld

Office of Naval Research (2 copies)
Department of the Navy
Code 01231C
Arlington, VA 22217

Office of Under Secretary of Defense
Research and Engineering
Room 3E1034
The Pentagon
Washington, DC 20301
Attn: Dr. John MacCallum

ORI, Inc.
1375 Piccard Drive
Rockville, MD 20850
Attn: Dr. C. M. Huddleston

Physics International, Inc.
2700 Merced Street
San Leandro, CA. 94577
Attn: Dr. E. Goldman

Princeton University
Plasma Physics Laboratory
Princeton, NJ 08540
Attn: Dr. Francis Perkins, Jr.

Pulse Sciences, Inc.
600 McCormack Street
San Leandro, CA 94577
Attn: Dr. Sidney Putnam
Dr. John Bayless

The Rand Corporation
2100 M Street, NW
Washington, DC 20037
Attn: Dr. Nikita Wells
Mr. Simon Kassel

Sandia National Laboratory
Albuquerque, NM 87115
Attn: Dr. David Hasti/1272
Dr. Collins Clark
Dr. Barbara Epstein
Dr. John Freeman/1241
Dr. Charles Frost
Dr. George Kamin/1274
Dr. Gordon T. Leifeste
Dr. Gerald N. Hays
Dr. James Chang
Dr. Michael G. Mazerakis/1272
Dr. John Wagner/1241
Dr. Ron Lipinski/1274

Science Applications Intl. Corp.
P. O. Box 2351
La Jolla, CA 92038
Attn: Dr. Rang Tsang

Science Applications Intl. Corp.
5150 El Camino Road
Los Altos, CA 94022
Attn: Dr. R. R. Johnston
Dr. Leon Feinstein
Dr. Douglas Keeley

University of Michigan
Dept. of Nuclear Engineering
Ann Arbor, MI 48109
Attn: Prof. Terry Kammash
Prof. R. Gilgenbach

Science Applications Intl. Corp.
1710 Goodridge Drive
McLean, VA 22102
Attn: Mr. W. Chadsey
Dr. A Drobot
Dr. K. Papadopoulos

Commander
Space & Naval Warfare Systems Command
PMW-145
Washington, DC 20363-5100
Attn: CAPT J. D. Fontana
LT Fritchie

SRI International
PS0-15
Molecular Physics Laboratory
333 Ravenswood Avenue
Menlo Park, CA 94025
Attn: Dr. Donald Eckstrom
Dr. Kenneth R. Stalder

Strategic Defense Initiative Org.
1717 H Street, N. W.
Washington, DC 20009
Attn: Lt Col R. L. Gullickson
Dr. J. Ionson
Dr. D. Duston

Strategic Defense Initiative Office
Directed Energy Weapons Office, The
Pentagon
Office of the Secretary of Defense
Washington, DC 20301-7100
Attn: Dr. C. F. Sharn (0P0987B)

Titan Systems, Inc.
9191 Towne Centre Dr.-Suite 500
San Diego, CA 92122
Attn: Dr. R. M. Dove

University of California
Physics Department
Irvine, CA 92664
Attn: Dr. Gregory Benford

University of Maryland
Physics Department
College Park, MD 20742
Attn: Dr. Y. C. Lee
Dr. C. Grebogi

Director of Research
U.S. Naval Academy
Annapolis, MD 21402 (2 copies)

Records (1 copy)